ABSTRACT

Angiogenesis Imaging of Myocardial Infarction Using ^{68}Ga-RGD PET: Characterization and Application to Therapeutic Efficacy Monitoring

Eo, Jae Seon

Seoul National University College of Medicine

Purpose: ^{68}Ga-RGD PET is a recentl developed molecular imaging modality that visualizes angiogenesis. In myocardial infarction (MI), angiogenesis is one of the key processes for understanding pathophysiology and implementing therapeutic interventions. In this study, ^{68}Ga-RGD PET was used to investigate imaging characteristics in a rat MI model, as well as to monitor experimental angiogenesis induction therapy.

Materials and methods: To assess imaging characteristics, 6 female Sprague-Dawley rats with MI induced by ligation of the left anterior descending artery (LAD) and 4 sham-operated rats were used. ^{68}Ga-RGD PET was performed on post-operative days (POD) 1, 7, and 14. ^{68}Ga-BAPEN PET and ^{18}F-FDG PET were also performed to evaluate perfusion and glucose metabolism, respectively. Results from ^{68}Ga-BAPEN PET and ^{18}F-FDG PET were also directly compared with those from ^{68}Ga-RGD PET. Quantitative analyses were performed by measuring the lesion-to-normal ratio (LNR) by drawing regions

of interest for the LAD territory and normal remote myocardium on ^{68}Ga-RGD PET. Autoradiography for ^{68}Ga-RGD and immunohistochemical (IHC) staining for VEGF and CD68 were performed to assess the mechanism of RGD accumulation. In order to monitor experimental angiogenesis induction therapy, an additional 7 rats underwent LAD ligation; 4 were injected with recombinant human basic fibroblast growth factor (rhbFGF), and the remaining 3 were injected with saline. ^{68}Ga-RGD PET was performed on POD 1, 7, and 14, and ^{18}F-FDG PET was performed on POD 2 and 15. PET images were compared with those of the 3 sham-operated rats.

Results: On PET images, ^{68}Ga-RGD uptake in the LAD territory was significantly increased in MI-induced rats compared with sham-operated rats from POD 1 (LNR 1.47±0.16 versus 1.13±0.14, P=0.010) through POD 14 (LNR 1.31±0.14 versus 1.06±0.07, P=0.019), and this uptake gradually decreased over time. The areas with increased ^{68}Ga-RGD uptake on POD 14 corresponded with the final infarct lesions that demonstrated metabolic defects on ^{18}F-FDG PET and perfusion defects on ^{68}Ga-BAPEN PET. Autoradiography also demonstrated ^{68}Ga-RGD uptake in the infarcted tissue. On IHC staining, ^{68}Ga-RGD uptake corresponded with VEGF expression and macrophage accumulation in the infarcted tissue. In monitoring angiogenesis induction therapy, the LNR on ^{68}Ga-RGD PET was 1.61±0.15 in the rhbFGF group on POD 1, which was significantly higher than that of saline-injected and sham-operated groups (1.37±0.06 and 1.17±0.14, respectively; P=0.018). However, no significant differences were observed at subsequent time points. Additionally, no significant differences were found between the rhbFGF and saline-injected groups with respect to final infarct size, degree of infarct change, autoradiography, or IHC results.

Conclusion: This study demonstrated the characteristics of ^{68}Ga-RGD PET as an angiogenesis imaging modality post-MI. In the monitoring of therapeutic efficacy of single injections of rhbFGF using ^{68}Ga-RGD PET, rhbFGF was effective for induction of short-term angiogenesis, though it had limited long-term effects. Thus, ^{68}Ga-RGD PET would be a useful angiogenesis imaging modality in MI for assessment of pathophysiology and monitoring of therapeutic efficacy.

Key Words: ^{68}Ga, RGD peptide, positron emission tomography, therapeutic angiogenesis, myocardial infarction

***Student Number*: 2006-30507**

List of Figures

List of Abbreviations and Symbols

Abbreviation	Full Name
LAD	Left anterior descending artery
MI	Myocardial infarction
bFGF	Basic fibroblast growth factor
RGD	Arginine-Glycine-Aspartate
MRI	Magnetic resonance imaging
NOTA	1,4,7-triazacyclononane-1,4,7-triacetic acid
PET	Positron emission tomography
CT	Computed tomography
BAPEN	tris (4,6-dimethoxysalicylaldimine)-N,N′-bis(3-aminopropyl)-N,N′-ethylenediamin
FDG	2- Fluoro -2- deoxy -D-glucose
FOV	Field of view
ROI	Region of interest
LNR	LAD territory-to-normal uptake ratio
POD	Post-operative day
rhbFGF	Recombinant human basic fibroblast growth factor
MI-FGF	Myocardial infarction with rhbFGF injection
MI-Saline	Myocardial infarction with saline injection
TTC	Triphenyltetrazolium chloride
H&E	Hematoxylin and eosin
VEGF	Vascular endothelial growth factor

Contents

Introduction

Cardiovascular diseases, including myocardial infarction (MI), are the most common cause of death worldwide In 2008, 7.3 million people died of ischemic heart disease (1). Among the many pathophysiological changes that occur in MI, angiogenesis is one of the key processes targeted for diagnosis and therapy. Angiogenesis is a natural repair processes that occurs after MI(2,3), thus therapeutic angiogenesis induction may reduce infarct size, increase collateral vessel formation, and improve left ventricular function (4). A molecular imaging modality for visualizing angiogenesis would be useful in diagnosing characteristics of MI and to monitor efficacy of angiogenesis induction therapy.

A tripeptide moiety of Arg-Gly-Asp (RGD) has been highlighted for use in angiogenesis imaging, as it specifically binds to $\alpha_v\beta_3$ integrin which is richly expressed in endothelial cells activated for angiogenesis. As a result, enhanced expression of $\alpha_v\beta_3$ integrin is commonly observed in ischemic lesions and malignant tumors (5). To develop molecular imaging probes for angiogenesis, RGD peptides had been combined with a signaling moiety. Nanotubes, quantum dots, paramagnetic particles and microbubbles combined with RGD peptides have been developed for optical imaging,

magnetic resonance imaging (MRI), and ultrasonography (5). For nuclear imaging, which is the most sensitive clinical molecular imaging modality, radiolabeled RGD derivatives have been developed using radioisotopes such as ^{99m}Tc, ^{18}F, ^{64}Cu, ^{111}In and ^{125}I (5–10).

Recently, a ^{68}Ga-labeled RGD agent based on 1,4,7-triazacyclononane-1,4,7-triacetic acid (NOTA) was developed (11). ^{68}Ga is a practical radioisotope for clinical positron emission tomography (PET) (12–14), as it is a positron emitter with a half-life of 68 minutes. Its short half-life is advantageous as it provides a low level of radiation exposure. Additionally, ^{68}Ga can be produced by a commercially available ^{68}Ge/^{68}Ga generator and does not require a cyclotron system, making it more accessible and less expensive. The long half-life (270.8 days) of the parent nuclide, ^{68}Ge, allows the generator to be clinically available for more than one year. ^{68}Ga-RGD is produced by labeling NOTA-RGD with ^{68}Ga, and previous studies have demonstrated that ^{68}Ga-RGD PET has acceptable levels of radiation exposure and adequate angiogenesis imaging capabilities in a mouse tumor model (11,14). Thus, ^{68}Ga-RGD PET may also have potential for application to angiogenesis imaging in cardiovascular disease.

The purpose of angiogenesis induction therapy is to induce formation of new blood vessels using drugs, gene therapy, or stem cell treatment. This method may be clinically useful for those patients who cannot undergo

bypass surgery or percutaneous coronary intervention. Despite advances in medical technology, more than 30% of coronary artery disease patients cannot undergo surgical or interventional reperfusion therapy (15). Basic fibroblast growth factor (bFGF) is one of the agents used in angiogenesis induction therapy, which may reduce infarct size, improve systolic function, and increase collateral circulation (4). Several animal studies have reported that bFGF treatment effectively improves function of the ischemic myocardium (15–20). With regard to angiogenesis, treatment with bFGF was reported to induce expression of $\alpha_v\beta_3$ integrin in endothelial cells (21).

In this study, the characteristics of ^{68}Ga-RGD PET as an angiogenesis imaging modality were assessed in a rat MI model. Additionally, monitoring of therapeutic efficacy for an experimental angiogenesis induction therapy using bFGF was evaluated.

Materials and Methods

Myocardial Infarction Animal Model

For the myocardial infarction rat model, female Sprague-Dawley rats (200–300g body weight) were obtained from the Center for Animal Resource Development at Seoul National University. The rats were anesthetized with an intraperitoneal injection of ketamine hydrochloride (100mg/kg, Yuhan Corp., Seoul, Korea) and xylazine (10mg/kg, Virbac Korea, Seoul, Korea), and were intubated and ventilated with positive-pressure room air using a rodent ventilator (Inspira ASV, Harvard Apparatus, Holliston, MA). A left-sided thoracotomy was performed through the fourth intercostal space, and the pericardium was opened. MI was induced by ligation of the left anterior descending artery (LAD) with 6-0 silk suture, as previously described (22). The chest wall was then closed in layers and the pneumothorax was evacuated. Sham-operation was performed using the same procedure except for ligation of the LAD. All animal experiments were approved by the Institutional Animal Care and Use Committee of the Seoul National University Hospital.

Preparation of ^{68}Ga-RGD and ^{68}Ga-BAPEN

^{68}Ga-RGD was prepared as previously described (11). In brief, SCN-Bn-NOTA and c(RGDyK) were purchased from Futurechem (Seoul, Korea). These were mixed and allowed to react for 20 hours in 0.1M Na_2CO_3 solution at room temperature. The reaction mixture was subsequently purified by high-performance liquid chromatography, and NOTA-RGD was collected. ^{68}Ga was eluted from a ^{68}Ge/^{68}Ga generator with 0.1M HCl and added to the NOTA-RGD kit. After a 10-minute incubation at room temperature, ^{68}Ga-RGD was purified using an Alumina N Sep-Pak® cartridge to remove ^{68}Ge and free ^{68}Ga. ^{68}Ga-tris(4,6-dimethoxysalicylaldimine)-N,N′-bis(3-aminopropyl)-N,N′-ethylenediamin (^{68}Ga-BAPEN) was used as a PET imaging agent to evaluate myocardial perfusion. ^{68}Ga-BAPEN was prepared with a synthesis kit as previously described (23).

PET Imaging Protocol

A dedicated small animal PET/CT scanner (eXplore Vista, GE Healthcare, USA) was used for ^{68}Ga-RGD, ^{68}Ga-BAPEN and ^{18}F-2-Fluoro-2-deoxy-D-glucose (FDG) PET imaging. Rats were anesthetized with 2% isoflurane, and ^{68}Ga-RGD (18.5MBq/0.1mL) was injected into the tail vein. PET scans started 30 minutes after injection and static PET images were

acquired for 30 minutes in a single position covering a 4.6cm field of view (FOV) from the neck to the liver. CT scan was subsequently performed for the same FOV. The acquired images were reconstructed by a 3-D ordered subset expectation maximization algorithm method with 16 iterations, combined with scatter and random corrections. Reconstructed PET images were displayed as trans-axial images fused with CT images. ^{68}Ga-BAPEN PET (18.5MBq/0.1mL) and CT scans were performed using the same protocol as that of ^{68}Ga-RGD PET. For ^{18}F-FDG PET/CT, rats were injected with ^{18}F-FDG (18.5MBq/0.1mL) into the tail vein, and a 30 minute static PET scan was begun 60 minutes after injection. Image acquisition and reconstruction methods were as described for the ^{68}Ga-RGD PET/CT scans. The overall protocols for the PET and CT scans are shown in Fig. 1.

Characteristics of ^{68}Ga-RGD PET in Myocardial Infarction

Six MI-induced and 4 sham-operated rats were used as subjects. ^{68}Ga-RGD PET was performed on post-operative days (POD) 1, 7, and 14. ^{18}F-FDG PET scans were done on POD 16 to visualize the infracted area with metabolic imaging. For evaluation of myocardial perfusion, ^{68}Ga-BAPEN PET was performed on POD 15 for 3 rats in each group. The overall imaging protocol for this study is shown in Fig. 3. To compare patterns of

angiogenesis and the area of infarction, the size of the lesions on ^{68}Ga-RGD and ^{18}F-FDG PET were compared.

For quantitative image analysis, all PET and CT images were converted to DICOM format, and images were analyzed using the AMIDE software package (24). To measure tissue uptake, regions of interest (ROIs) were drawn for the LAD territory and the remote normal myocardium. Three ROIs were drawn on the ^{68}Ga-RGD PET/CT fusion images, and counts for all ROIs were averaged. Finally, the mean uptake of each region was expressed as mean count per pixel in the ROIs. LAD territory-to-normal uptake ratios (LNRs) were calculated as mean uptake in the LAD territory divided by mean uptake in the remote myocardium. An example of the drawn ROIs and calculated LNR is shown in Fig. 2. In the analyses, background CT images were used as reference images for localization of uptake on PET.

Efficacy Monitoring of Angiogenesis Therapy Using ^{68}Ga-RGD PET

Angiogenesis induction therapy was performed using recombinant human basic fibroblastic growth factor (rhbFGF). MI was induced in 7 rats using the methods described above, and rhbFGF (20μg/0.1mL, Sino Biological Inc., Beijing, China) was injected into the peri-infarcted area via intramyocardial injection after ligation of the LAD (19,25) in 4 rats (MI-

FGF group). The remaining 3 rats were injected with normal saline (MI-saline group). Additionally, 3 rats were sham-operated without MI induction (sham group). For these subjects, ^{68}Ga-RGD PET was performed on POD 1, 7, and 14, with the same protocol as previously described. For evaluation of infarct size, ^{18}F-FDG PET scans were done on POD 2 and 15. The overall imaging protocol is shown in Fig. 4.

Autoradiography and Histopathologic Study

Autoradiography and histopathology for ^{68}Ga-RGD was performed in each rat after completion of the final PET scan (POD 19–28). Thirty minutes after injection of ^{68}Ga-RGD (185MBq) into the tail vein, the rat was sacrificed and the heart was dissected. A radiosensitive image plate was exposed to a short-axis slice of the myocardium for 2 hours, and was subsequently analyzed using a BAS 1500 system (Fuji, Tokyo, Japan). To confirm that a MI occurred, 2,3,5-triphenyltetrazolium chloride (TTC) staining of the myocardium was performed in addition to hematoxylin and eosin (H&E) staining.

Immunohistochemistry (IHC) staining was done for vascular endothelial growth factor (VEGF) and CD68 to assess the mechanism of ^{68}Ga-RGD uptake. VEGF and CD68 were used as markers for activation of angiogenesis and macrophage accumulation, respectively (26). Murine

anti-VEGF antibody and anti-CD68 antibody (Abcam plc., UK) were used for the staining.

Statistical Analysis

All of the quantitative data are expressed as the mean ± SD. In the group comparisons of uptake ratios, ANOVAs using rank tests (Kruskal-Wallis test and Mann-Whitney U test) were used. The Wilcoxon signed rank test was performed for comparisons of values obtained on POD 1, 7, and 14. *P*-values <0.05 were considered to be statistically significant. Statistical analyses were performed using a commercial statistics software package (SPSS Statistics 17.0, IBM, Armonk, NY).

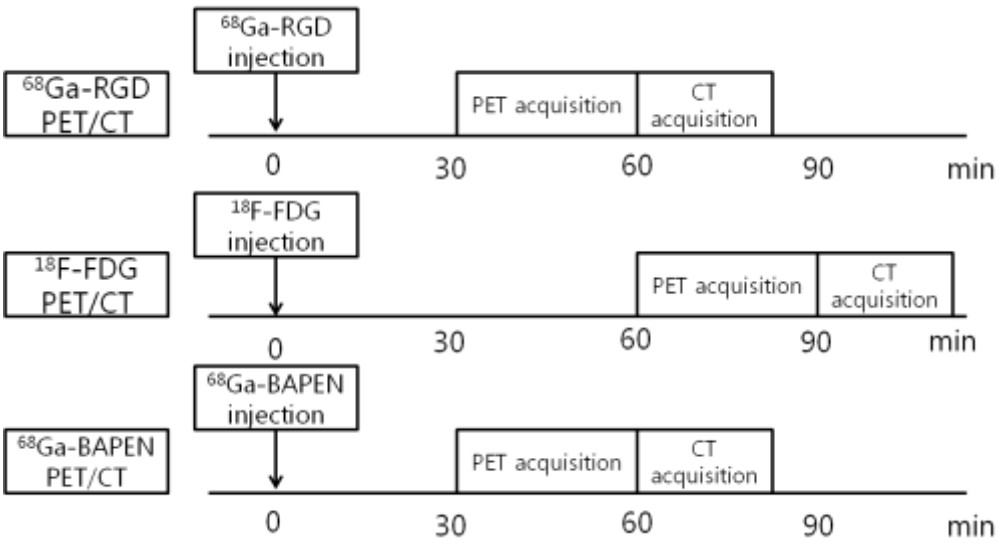

Fig. 1. Imaging protocol for ^{68}Ga-RGD, ^{68}Ga-BAPEN and ^{18}F-FDG PET

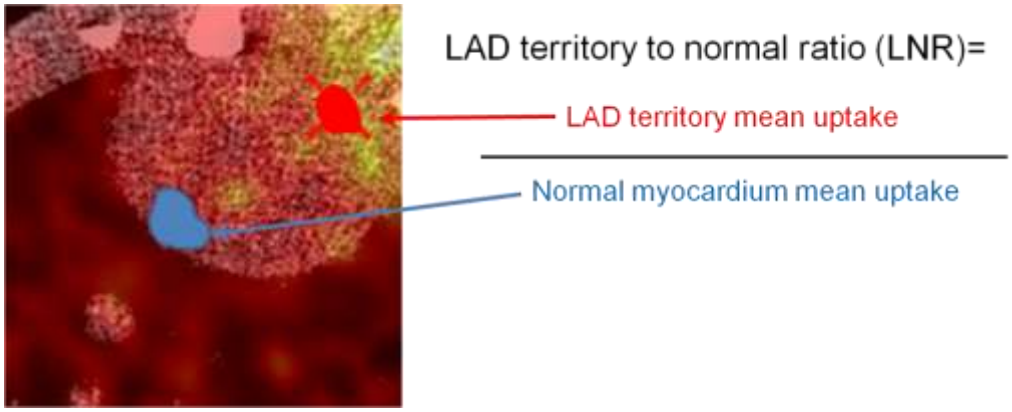

Fig. 2. Examples of regions of interest drawn for the infarcted LAD territory and normal remote myocardium. LNR was calculated as the ratio of mean uptakes between the 2 regions.

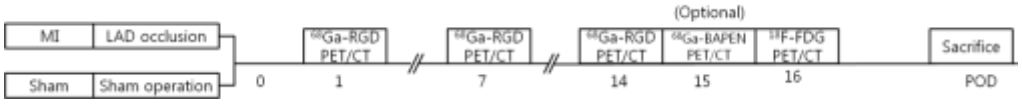

Fig. 3. Overall study protocol to assess imaging characteristics of ^{68}Ga-RGD PET in an MI model

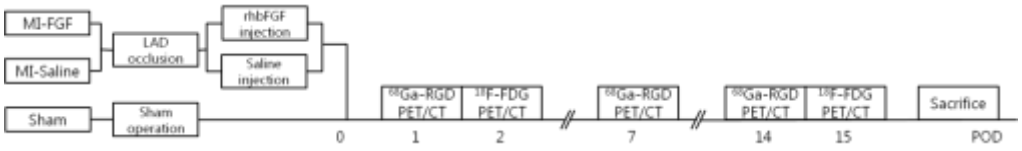

Fig. 4. Overall study protocol to monitor therapeutic efficacy of rhbFGF therapy using ^{68}Ga-RGD PET

Results

Characteristics of ^{68}Ga-RGD PET after Myocardial Infarction

In the infarcted LAD territory of the myocardium, increased ^{68}Ga-RGD uptake was observed on PET images from POD 1 through POD 14. In contrast, no definite increase in ^{68}Ga-RGD uptake was observed in sham-operated myocardium. Regions of ^{68}Ga-RGD uptake corresponded with final infarct lesions that demonstrated metabolic defects on ^{18}F-FDG and perfusion defects on ^{68}Ga-BAPEN PET (Fig. 5).

In quantitative analyses, the LNR of the infarcted myocardium was significantly higher than that of sham-operated myocardium on POD 1 (1.47±0.16 versus 1.13±0.14, P=0.010). On POD 7 and 14, the LNRs were also significantly higher in the infarcted myocardium than the sham-operated myocardium (1.38±0.18 versus 1.07±0.06, P=0.010; and 1.31±0.14 versus 1.06±0.07, P=0.019, respectively). Uptake in the infarcted myocardium, however, gradually decreased with time, as the LNR on POD 14 was significantly lower than on POD 1 (P=0.028, Fig. 6).

The area of infarcted myocardium with increased ^{68}Ga-RGD uptake seen on POD 1 was smaller than the final infarcted region demonstrated by ^{18}F-FDG PET. The area of increased ^{68}Ga-RGD uptake on POD 14, however, was similar to the final infarct lesion (Fig. 7).

Autoradiography and Histopathology

Successful induction of MI was confirmed by histopathologic studies. On H&E staining, thinning with fibrotic change was observed in the infarcted region in the distal portion of the ligated LAD territory. Additionally, unstained white fibrotic tissue was observed on TTC staining. The regions of increased ^{68}Ga-RGD uptake on autoradiography matched with the infracted region, including the penumbra region (Fig. 8).

IHC staining demonstrated increased expression of VEGF and CD68 in the infarcted myocardium compared with normal myocardium (Fig. 9). There were no significant differences in VEGF and CD68 expression between MI-FGF and MI-saline groups. In contrast, enhanced expression of VEGF and CD68 was not observed in the sham-operated myocardium.

Efficacy Monitoring of Angiogenesis Therapy Using ^{68}Ga-RGD PET

In both the MI-FGF and MI-saline groups, ^{68}Ga-RGD uptake was increased in the infarcted myocardium from POD 1 through POD 14, and this uptake gradually decreased with time (Fig. 10). On POD 1, the LNR of the MI-FGF group was 1.61±0.15, which was significantly higher than that of the MI-saline (1.37±0.06) and sham groups (1.17±0.14, P=0.018). This effect was not sustained, however, and no significant differences in LNR between the MI-FGF and MI-saline groups were observed on POD 7

(1.45±0.13 versus 1.44±0.09, *P*=n.s.) or POD 14 (1.29±0.08 versus 1.23±0.01, *P*=n.s.) (Fig. 11).

When the size of the infarct was assessed on ^{18}F-FDG PET, no significant changes were observed between POD 2 and 15 in either the MI-FGF or MI-saline groups (Fig. 12).

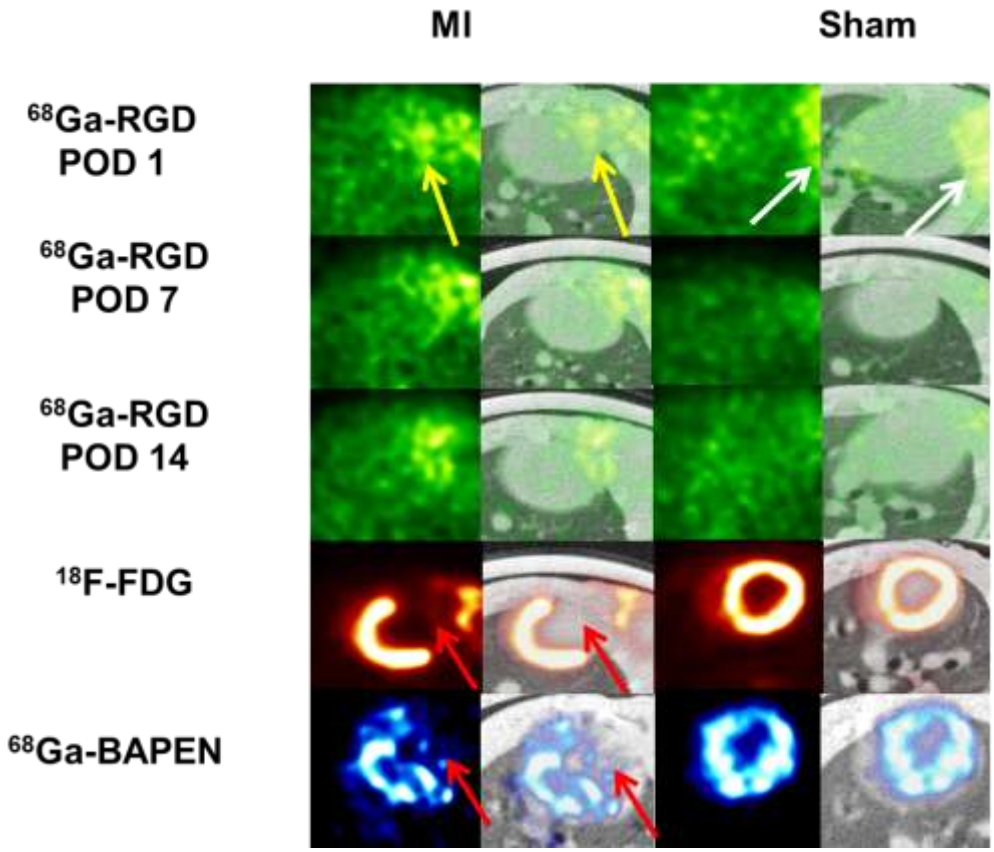

Fig. 5. Time course of ^{68}Ga-RGD PET imaging after MI. ^{68}Ga-RGD uptake in the LAD territory was increased from POD 1 through POD 14, and gradually decreased with time (yellow arrow). No significant uptake existed in sham-operated myocardium. The region of ^{68}Ga-RGD uptake in MI corresponded with metabolic defects on ^{18}F-FDG PET and perfusion defects on ^{68}Ga-BAPEN PET (red arrow). Sham-operated myocardium showed no defects in metabolism or perfusion. ^{68}Ga-RGD uptake in the chest wall was observed as a post-operative change (white arrow).

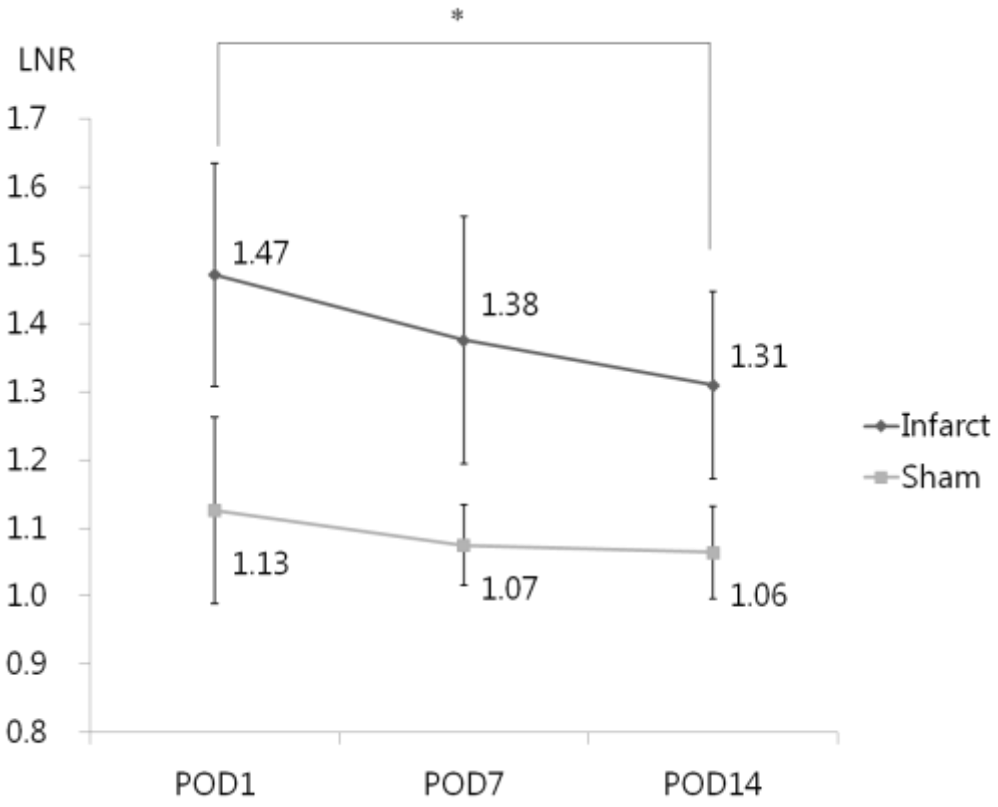

Fig. 6. Time course of ^{68}Ga-RGD uptake in MI and sham-operated myocardium. The LNRs of the MI group were significantly higher than those of the sham-operated group on POD 1, 7, and 14 (P=0.010, 0.010, and 0.019, respectively). The LNR of the MI group was significantly decreased on POD 14 compared with POD 1 (asterisk, P=0.028).

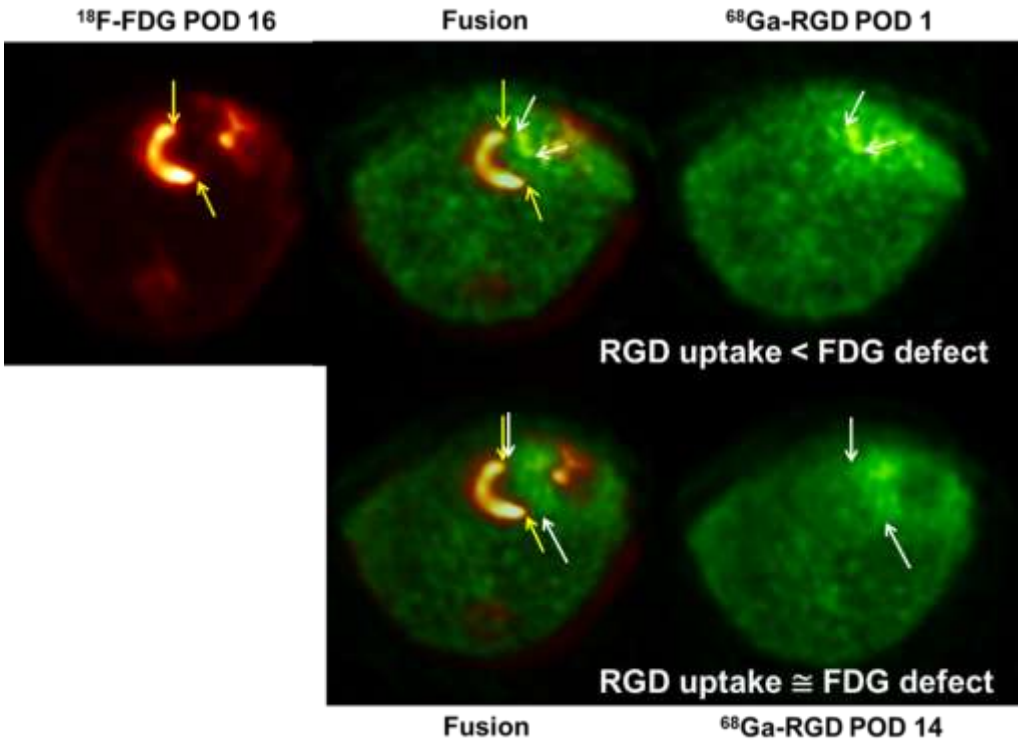

Fig. 7. Comparison of ^{68}Ga-RGD and ^{18}F-FDG PET images after MI. The area of infarcted myocardium showed intensely increased ^{68}Ga-RGD uptake on POD 1 (white arrow), and was smaller than the final defect on ^{18}F-FDG PET (yellow arrow). On POD 14, ^{68}Ga-RGD uptake was mild and diffuse in the infarcted myocardium which closely corresponded with the defect seen on ^{18}F-FDG PET.

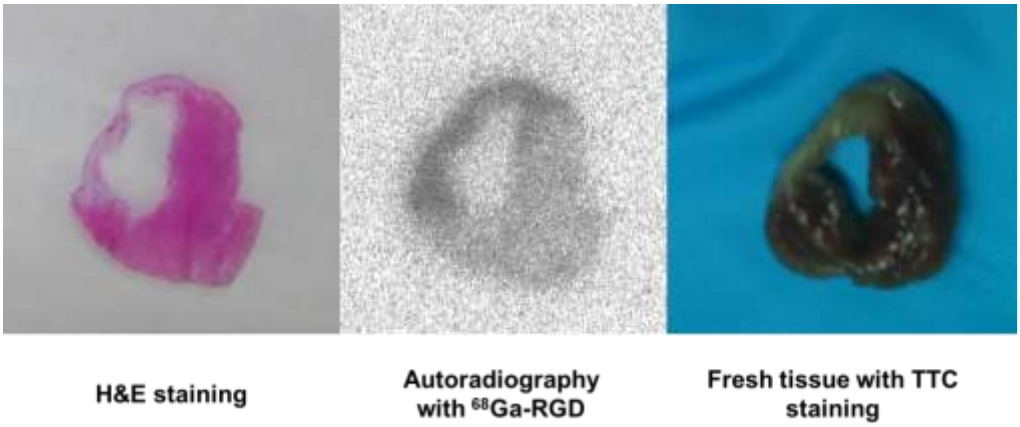

Fig. 8. Autoradiography and histopathology of ^{68}Ga-RGD in MI. Increased ^{68}Ga-RGD uptake was visualized on autoradiography and matched with the infarcted region on TTC staining and thinned fibrotic scar on H&E staining. The penumbra region also demonstrated increased ^{68}Ga-RGD uptake.

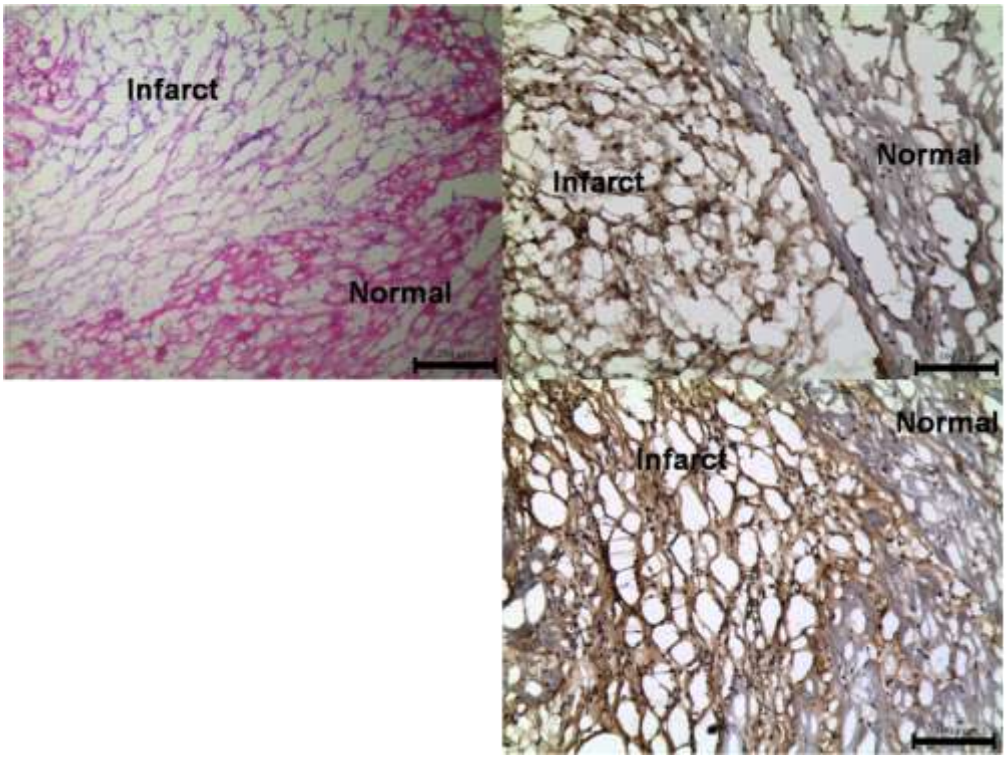

Fig. 9. Immunohistochemistry staining for VEGF and CD68. H&E staining (left upper), immunohistochemistry staining for CD68 (right upper), and VEGF (right lower) are shown. The expression of VEGF and CD68 were increased in the infarcted myocardium, demonstrating the mechanism of ^{68}Ga-RGD uptake.

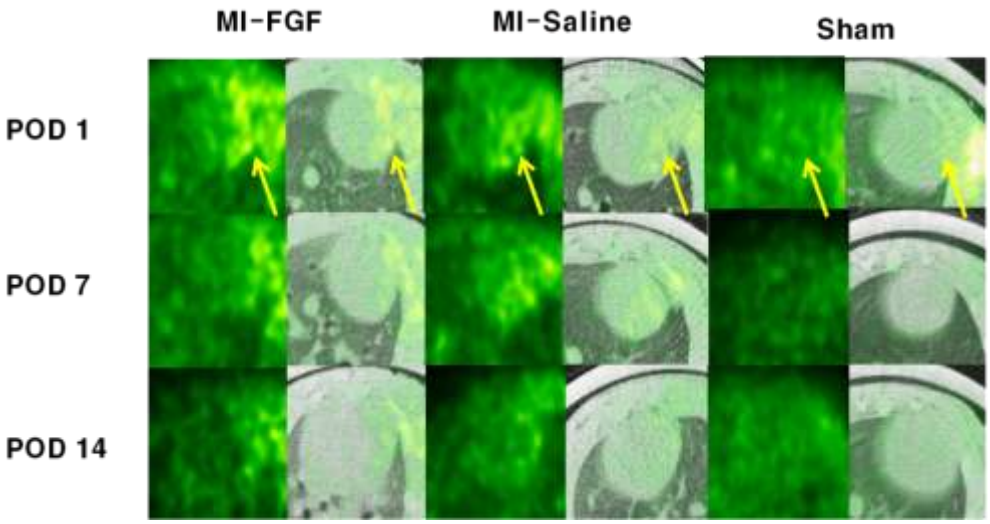

Fig. 10. ^{68}Ga-RGD PET images for therapeutic efficacy monitoring in rhbFGF treatment. Greater increases in ^{68}Ga-RGD uptake in the LAD territory was observed in the MI-FGF group than in the MI-saline or sham groups (yellow arrow). Uptake gradually decreased with time in all three groups. ^{68}Ga-RGD uptake in the chest wall was observed as a post-operative change.

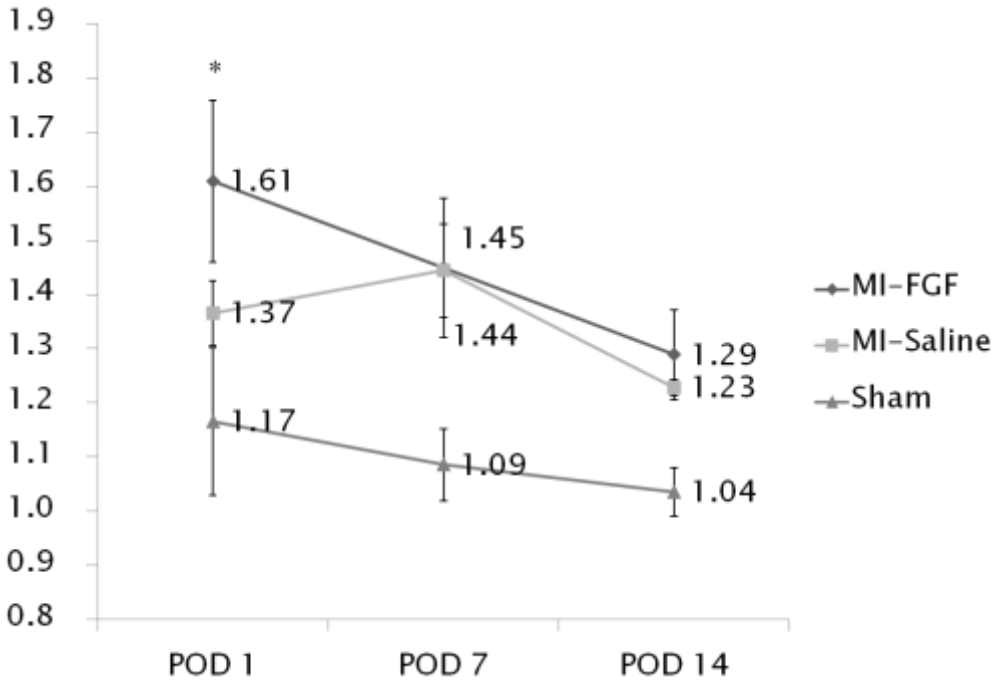

Fig. 11. Time course of ^{68}Ga-RGD uptake in rhbFGF treatment. On POD 1, ^{68}Ga-RGD uptake was significantly higher in the MI-FGF group compared with MI-saline and sham groups (P=0.018). However, no significant differences existed between groups on POD 7 and 14.

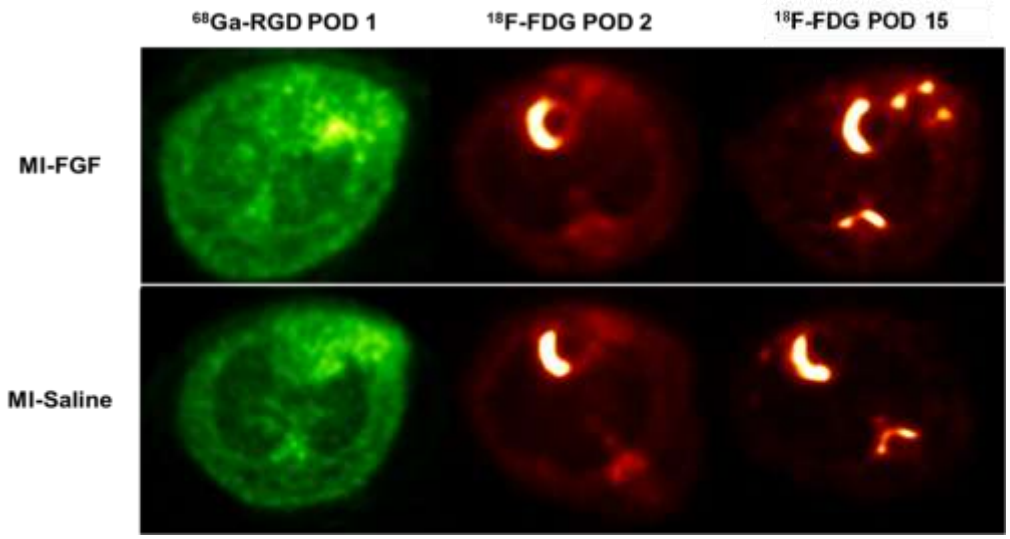

Fig. 12. Changes in the size of the infarct between POD 2 and POD 15. Considering compensatory enlargement of the left ventricle, the infarct size on POD 15 was similar to that of POD 2 in the MI-FGF and MI-saline groups. The difference in infarct size between the MI-FGF and the MI-saline groups was not significant.

Discussion

In the current study, ^{68}Ga-RGD PET demonstrated increased uptake in the infarcted myocardium, which corresponded with enhanced angiogenesis and macrophage accumulation. ^{68}Ga-RGD uptake intensity was gradually decreased with time whereas the area of increased uptake extended, finally matching with the infarcted region. In monitoring the efficacy of angiogenesis induction therapy, rhbFGF treatment induced angiogenesis on POD 1, but further increases in angiogensis were not observed on subsequent PODs. Additionally, no significant differences were observed in changes in infarct size between rhbFGF-treated and non-treated groups.

Angiogenesis is one of the natural repair mechanisms that restores perfusion of ischemic tissue after MI, and is related to post-infarct cardiac remodeling and prognosis (2). Thus, assessment of angiogenic activity in MI would be helpful with regard to the pathophysiologic state of disease and determining the prognosis of the patient. For angiogenesis imaging, an RGD peptide that specifically binds to $\alpha_v\beta_3$ integrin is an effective target moiety (5). $\alpha_v\beta_3$ integrin is the most abundant integrin on the surface of proliferating endothelial cells, and has been implicated in cell migration and signaling for cell survival. Several imaging probes using RGD peptide

have been developed (5–10), and ^{68}Ga-RGD, a positron-emitting RGD agent, was used for angiogenesis PET imaging in this study.

On autoradiography, ^{68}Ga-RGD uptake was increased in the infarcted myocardium as confirmed by H&E and TTC staining. In contrast, the sham-operated myocardium did not show any increases in uptake. Additionally, ^{68}Ga-RGD uptake on PET imaging was demonstrated in the infarcted myocardium on POD 1, and gradually decreased over time through POD 14. Rodriguez et al. investigated the use of PET for angiogenesis imaging using VEGF receptors in a rat MI model (27). In that study, serial PET scans showed enhanced angiogenesis in the infarcted tissue for 2 weeks post-MI, which ultimately returned to baseline. These results are consistent with those reported in the current study.

Intriguingly, ^{68}Ga-RGD uptake was also observed in the penumbra region on autoradiography. Since autoradiography was performed after POD 17, this finding is classified as subacute. On PET images, the area of increased ^{68}Ga-RGD uptake on POD 1 was smaller than the final infarct area on ^{18}F-FDG PET. The area of increased ^{68}Ga-RGD uptake gradually extended with time and corresponded with the final infarct region on POD 14. The mismatched region on POD 1 would be risky myocardium in acute stage of infarct, because it finally turned out to be infarcted myocardium, although angiogenesis of the region was activated on POD 14. If

angiogenesis in the region had been induced early in acute stage, the region would have been salvaged from infarction. Thus, further research is warranted on the salvage effect of angiogenesis induction therapy.

In our IHC experiment, which was performed to assess the mechanism of ^{68}Ga-RGD uptake, enhanced expression of VEGF and CD68 was observed in the infarcted region where ^{68}Ga-RGD uptake was increased. It is well known that expression of $\alpha_v\beta_3$ integrin is enhanced on the surface of angiogenic endothelial cells with macrophage activation (28). Thus, angiogenic activation and inflammatory macrophage accumulation in the infarcted myocardium are likely the primary mechanisms of ^{68}Ga-RGD uptake. Inflammation due to macrophage accumulation also plays an important role in the pathophysiology of MI (29). Induction of angiogenesis by growth factors results in inflammatory-like reactions such as vasodilatation, increased permeability, and accumulation of monocytes and macrophages (28). Although ^{68}Ga-RGD uptake is not highly specific for angiogenesis alone, it allows for visualization of important inflammatory effects.

Despite the intriguing characteristics of ^{68}Ga-RGD PET, this method has limited sensitivity. Although significant differences existed between MI and sham-operated groups, the signal-to-noise ratio on ^{68}Ga-RGD PET was low and the measured TNR was 1.47-1.31 in the MI group. These values

are unsatisfactory for clinical application. In order to amplify the signal, dimers or tetramers of the RGD peptide could be considered as alternative agents that may have a higher affinity for integrin than the RGD monomer (30).

The most effective treatment option for ischemic heart disease is reperfusion therapy, with surgical and interventional reperfusion therapies being the main treatment options for chronic coronary artery disease and MI. In patients who cannot receive reperfusion therapy, however, angiogenesis induction therapy as well as medical management may be another useful treatment option (16). Angiogenesis induction therapy includes use of angiogenic drugs as well as gene and cell therapy for neovascularization. Many angiogenesis induction therapies have been investigated, though bFGF is one of the most widely studied agents for neoangiogenesis. In a canine MI model, Yanagisawa-Miwa et al. reported that intracoronary infusion of bFGF reduced infarct size, increased collateral vessel formation, and improved left ventricular systolic function after 1 week in comparison with the control group (4). Additionally, in rat ischemia/reperfusion models, bFGF infusion resulted in reduction of infarct size (19,31). In a clinical trial of bFGF treatment during CABG, high-dose bFGF treatment induced a decrease in the size of the myocardial perfusion defect (32). In a long-term 32 month follow-up study, bFGF treatment

resulted in significantly lower occurrences of angina, lower stress perfusion defect scores, and higher late ventricular ejection fraction than that seen in the placebo group (33).

The long-term effects of bFGF on prognosis, however, is still controversial. Scheinowitz et al. continuously administered bFGF and insulin-like growth factor into the peritoneum in 72 rats subjected to acute MI. After 6 weeks, cross-sectional slices of the left ventricle showed no histopathological differences between the treated and control groups (34). Inagaki et al. also reported that intramyocardial injection of bFGF in rats with acute MI did not improve the regional myocardial blood flow, number of viable myocardial cells, or the extent of myocardial fibrosis 4 weeks later (35). Additionally, a multicenter, randomized, double-blind, placebo-controlled study using bFGF demonstrated a limited effect of treatment, with no significant difference existed in exercise tolerance, adverse effects and stress nuclear imaging, between bFGF treated and placebo groups 90 and 180 days after administration (36).

In this study, angiogenic activity on ^{68}Ga-RGD PET and metabolic defects shown by ^{18}F-FDG PET were not significantly different between bFGF-treated and saline-treated groups 2 weeks after injection. There were no significant differences between the two groups in change in infarction size on ^{18}F-FDG PET, IHC, or autoradiography. This result may be due to

the relatively short half-life of bFGF and its diminished effect in the presence of endothelial dysfunction (20). If bFGF remained in the myocardium for a longer period of time, the prognosis might be improved, as intramyocardial sustained delivery of bFGF has previously succeeded in improving angiogenesis and ventricular function in a rat MI model (37).

In the current study, ^{68}Ga-RGD PET was used as a monitoring method for therapeutic efficacy and demonstrated that even a single injection of bFGF has some effect. ^{68}Ga-RGD uptake was significantly higher in the bFGF-treated group than the saline-treated group on POD 1, although this difference was absent on POD 7 and 14. This implies that angiogenic activity in the infarcted myocardium was amplified shortly after bFGF injection, but was not sustained. Thus, a single injection of bFGF may be effective in the acute stage of MI in preparation for other treatment options. In this case, ^{68}Ga-RGD PET is an effective tool for efficacy monitoring of angiogenesis induction therapy.

^{18}F-FDG and ^{68}Ga-BAPEN PET, the gold standards for imaging in MI, were used in the current study. ^{68}Ga-BAPEN was introduced as a myocardial perfusion imaging agent for PET (38). Defects in perfusion and metabolism were regarded as infarcted myocardium.

The current study has several limitations. First, the number of subjects used in this experiment was relatively small, however, statistical

significance was demonstrated. Additionally, ^{68}Ga-RGD uptake in the chest wall due to inflammation was in close proximity to the infarcted myocardium and may have influenced quantification. Delineation of ROI was based on the combined CT images to distinguish ^{68}Ga-RGD activity of the infarcted myocardium from that of the chest wall.

Conclusion

This study demonstrated that ^{68}Ga-RGD PET is an effective method for angiogenesis imaging in MI. Additionally, ^{68}Ga-RGD PET was applied successfully to efficacy monitoring of an experimental angiogenic therapy. Thus, ^{68}Ga-RGD PET could be used as an effective angiogenesis imaging method in MI for diagnosis of the pathophysiologic state or efficacy monitoring of angiogenesis induction therapy.

.

References

1. WHO | The top 10 causes of death [Internet]. WHO. [cited 2012 Jan 21]. Available from: http://www.who.int/mediacentre/factsheets/fs310/en/index2.html

2. Oostendorp M, Douma K, Wagenaar A, et al. Molecular magnetic resonance imaging of myocardial angiogenesis after acute myocardial infarction. *Circulation*. 2010;121:775–83.

3. Hashimoto E, Ogita T, Nakaoka T, et al. Rapid induction of vascular endothelial growth factor expression by transient ischemia in rat heart. *Am J Physiol*. 1994;267:H1948–1954.

4. Yanagisawa-Miwa A, Uchida Y, Nakamura F, et al. Salvage of infarcted myocardium by angiogenic action of basic fibroblast growth factor. *Science*. 1992;257:1401–3.

5. Dobrucki LW, de Muinck ED, Lindner JR, Sinusas AJ. Approaches to multimodality imaging of angiogenesis. *J Nucl Med*. 2010;51 Suppl 1:66S–79S.

6. Dimastromatteo J, Riou LM, Ahmadi M, et al. In vivo molecular imaging of myocardial angiogenesis using the $\alpha_v\beta_3$ integrin-targeted tracer ^{99m}Tc-RAFT-RGD. *J Nucl Cardiol*. 2010;17:435–43.

7. Higuchi T, Bengel FM, Seidl S, et al. Assessment of αvβ3 integrin expression after myocardial infarction by positron emission tomography. *Cardiovasc Res*. 2008;78:395–403.

8. Li Z-B, Cai W, Cao Q, et al. ^{64}Cu-labeled tetrameric and octameric RGD peptides for small-animal PET of tumor $\alpha_v\beta_3$ integrin expression. *J Nucl Med*. 2007;48:1162–71.

9. Harris TD, Kalogeropoulos S, Nguyen T, et al. Design, synthesis, and evaluation of radiolabeled integrin alpha v beta 3 receptor antagonists for tumor imaging and radiotherapy. *Cancer Biother Radiopharm*. 2003;18:627–41.

10. Lee K-H, Jung K-H, Song S-H, et al. Radiolabeled RGD uptake and alphav integrin expression is enhanced in ischemic murine hindlimbs. *J Nucl Med*. 2005;46:472–8.

11. Jeong JM, Hong MK, Chang YS, et al. Preparation of a promising angiogenesis PET imaging agent: ^{68}Ga-labeled c(RGDyK)-isothiocyanatobenzyl-1,4,7-triazacyclononane-1,4,7-triacetic acid and feasibility studies in mice. *J Nucl Med*. 2008;49:830–6.

12. Shetty D, Lee YS, Jeong JM. ^{68}Ga-Labeled Radiopharmaceuticals for Positron Emission Tomography. *Nucl Med Mol Imaging*. 44:233–40.

13. Breeman WAP, Verbruggen AM. The ^{68}Ge/^{68}Ga generator has high potential, but when can we use ^{68}Ga-labelled tracers in clinical routine? *Eur J Nucl Med Mol Imaging*. 2007;34:978–81.

14. Kim JH, Lee JS, Kang KW, et al. Whole-Body Distribution and Radiation Dosimetry of ^{68}Ga-NOTA-RGD, a Positron Emission Tomography Agent for Angiogenesis Imaging. *Cancer Biotherapy & Radiopharmaceuticals* [Internet]. 2011 [cited 2012 Jan 21]; Available from: http://www.ncbi.nlm.nih.gov/pubmed/22149685

15. Boodhwani M, Sellke FW. Therapeutic Angiogenesis in Diabetes and Hypercholesterolemia: Influence of Oxidative Stress. *Antioxid Redox Signal*. 2009;11:1945–59.

16. Lassaletta AD, Chu LM, Sellke FW. Therapeutic neovascularization for coronary disease: current state and future prospects. *Basic Res Cardiol*. 2011;106:897–909.

17. Nishida S, Nagamine H, Tanaka Y, Watanabe G. Protective effect of basic fibroblast growth factor against myocyte death and arrhythmias in acute myocardial infarction in rats. *Circ J*. 2003;67:334–9.

18. Battler A, Scheinowitz M, Bor A, et al. Intracoronary injection of basic fibroblast growth factor enhances angiogenesis in infarcted swine myocardium. *J Am Coll Cardiol*. 1993;22:2001–6.

19. Xiao J, Lv Y, Lin S, et al. Cardiac protection by basic fibroblast growth factor from ischemia/reperfusion-induced injury in diabetic rats. *Biol Pharm Bull*. 2010;33:444–9.

20. Ahn A, Frishman WH, Gutwein A, Passeri J, Nelson M. Therapeutic angiogenesis: a new treatment approach for ischemic heart disease--Part II. *Cardiol Rev*. 2008;16:219–29.

21. Giancotti FG, Ruoslahti E. Integrin signaling. *Science*. 1999;285:1028–32.

22. Lee EJ, Choi E-K, Kang SK, et al. N-cadherin Determines Individual Variations in the Therapeutic Efficacy of Human Umbilical Cord Blood-derived Mesenchymal Stem Cells in a Rat Model of Myocardial Infarction. *Mol Ther*. 2012;20:155–67.

23. Yang BY, Jeong JM, Kim YJ, et al. Formulation of ^{68}Ga BAPEN kit for myocardial positron emission tomography imaging and biodistribution study. *Nucl Med Biol*. 2010;37:149–55.

24. Loening AM, Gambhir SS. AMIDE: a free software tool for multimodality medical image analysis. *Mol Imaging*. 2003;2:131–7.

25. Chang S-A, Lee EJ, Kang H-J, et al. Impact of myocardial infarct proteins and oscillating pressure on the differentiation of mesenchymal stem cells: effect of acute myocardial infarction on stem cell differentiation. *Stem Cells*. 2008;26:1901–12.

26. Kunisch E, Fuhrmann R, Roth A, et al. Macrophage specificity of three anti-CD68 monoclonal antibodies (KP1, EBM11, and PGM1) widely used for immunohistochemistry and flow cytometry. *Ann Rheum Dis*. 2004;63:774–84.

27. Rodriguez-Porcel M, Cai W, Gheysens O, et al. Imaging of VEGF Receptor in a Rat Myocardial Infarction Model Using PET. *J Nucl Med*. 2008;49:667–73.

28. Ahn A, Frishman WH, Gutwein A, Passeri J, Nelson M. Therapeutic angiogenesis: a new treatment approach for ischemic heart disease--part I. *Cardiol Rev*. 2008;16:163–71.

29. Minami E, Castellani C, Malchodi L, et al. The role of macrophage-derived urokinase plasminogen activator in myocardial infarct repair: urokinase attenuates ventricular remodeling. *J Mol Cell Cardiol*. 2010;49:516–24.

30. Dijkgraaf I, Yim C-B, Franssen GM, et al. PET imaging of αvβ3 integrin expression in tumours with ^{68}Ga-labelled mono-, di- and tetrameric RGD peptides. *Eur J Nucl Med Mol Imaging*. 2011;38:128–37.

31. Garbern JC, Minami E, Stayton PS, Murry CE. Delivery of basic fibroblast growth factor with a pH-responsive, injectable hydrogel to improve angiogenesis in infarcted myocardium. *Biomaterials*. 2011;32:2407–16.

32. Laham RJ, Sellke FW, Edelman ER, et al. Local perivascular delivery of basic fibroblast growth factor in patients undergoing coronary bypass surgery: results of a phase I randomized, double-blind, placebo-controlled trial. *Circulation*. 1999;100:1865–71.

33. Ruel M, Laham RJ, Parker JA, et al. Long-term effects of surgical angiogenic therapy with fibroblast growth factor 2 protein. *J Thorac Cardiovasc Surg*. 2002;124:28–34.

34. Scheinowitz M, Abramov D, Kotlyar A, Savion N, Eldar M. Continuous administration of insulin-like growth factor-I and basic fibroblast growth factor does not affect left ventricular geometry after acute myocardial infarction in rats. *Int J Cardiol*. 1998;63:217–21.

35. Inagaki M, Kimura A, Miyataka M, Ishikawa K. Basic fibroblast growth factor caused no change in collateral flow or infarct size of acutely-infarcted myocardium in rats. *Tohoku J Exp Med*. 2000;191:101–11.

36. Simons M, Annex BH, Laham RJ, et al. Pharmacological treatment of coronary artery disease with recombinant fibroblast growth factor-2: double-blind, randomized, controlled clinical trial. *Circulation*. 2002;105:788–93.

37. Iwakura A, Fujita M, Kataoka K, et al. Intramyocardial sustained delivery of basic fibroblast growth factor improves angiogenesis and ventricular function in a rat infarct model. *Heart Vessels*. 2003;18:93–9.

38. Tsang BW, Mathias CJ, Green MA. A gallium-68 radiopharmaceutical that is retained in myocardium: ^{68}Ga[(4,6-MeO2sal)2BAPEN]+. *J Nucl Med*. 1993;34:1127–31.

국문 초록

심근경색에서 ^{68}Ga-RGD PET 을 이용한 혈관신생영상: 특성평가 및 치료효과 평가에의 적용

어 재 선

서울대학교대학원 의학과 핵의학 전공

목적: 최근 개발된 ^{68}Ga-RGD PET 은 혈관신생을 표적으로 하는 분자영상법으로서, 심근경색에서 발현되는 혈관신생이나 최근 각광 받는 혈관신생치료 등의 모니터링에 유용할 것으로 기대되고 있다. 이 연구에서는 심근경색에서 ^{68}Ga-RGD 의 섭취 양상의 시간경과를 조사하고, 경색심근 영상 및 혈관신생치료 후 모니터링 영상법으로서의 가능성을 평가하고자 한다.

방법: 7 주령 암컷 Sprague-Dawley 쥐를 실험대상으로 하여 좌전하행관상동맥을 결찰하여 심근경색 모델을 만들었다. 심근경색 섭취양상 조사를 위해 6 마리 경색모델과 4 마리 위수술 시행 동물들에게서 시술 후 1 일, 7 일, 14 일째 ^{68}Ga-RGD, 15 일째 ^{68}Ga-BAPEN, 16 일째 ^{18}F-FDG 를 주사하고 PET/CT 를 촬영하였다. ^{68}Ga-RGD PET/CT 에서 경색심근-정상심근의 섭취 비율(LNR)을 구하여 정량비교를 하였다. 혈관신생치료

평가를 위해 네 마리에서 관상동맥 결찰 후 recombinant human basic fibroblast growth factor (bFGF)를 심근에 주입하였다. 세 마리는 bFGF 대신 생리식염수를 대신 주입하였고 다른 세 마리는 위수술을 실시하였다. 이들에게서 시술 후 1 일, 7 일, 14 일째에 ^{68}Ga-RGD PET/CT 를 촬영하였고 2 일, 15 일째에 ^{18}F-FDG PET/CT 를 촬영하였다. ^{68}Ga-RGD PET 에서 LNR 을 측정하고 ^{18}F-FDG PET/CT 영상에서 경색범위를 측정하여 비교하였다. 모든 개체에서 마지막 촬영이 끝난 후 ^{68}Ga-RGD 를 이용한 자가방사촬영과 H&E, TTC 염색, CD68 항체, VEGF 항체를 이용한 면역병리염색을 실시하였다.

결과: 경색심근 쥐의 경색영역에서 ^{18}F-FDG 와 ^{68}Ga-BAPEN 섭취 감소가 동반되어 성공적인 경색 유발을 확인하였고, 해당 부위에서 ^{68}Ga-RGD 섭취 증가가 경색유발 후 1 일에서 14 일의 전 기간에 걸쳐서 나타났다 ($p = 0.010, 0.019$). 자가방사촬영에서 경색심근에 ^{68}Ga-RGD 섭취가 확인되었으며 해당 부위는 VEGF 와 CD68 발현증가가 나타났다. 경색심근영역에서 bFGF 를 투여하여 혈관신생치료를 시행한 군들에서는 술후 1 일째의 RGD 섭취증가가 다른 군에 비해 유의하게 높았다. 그러나 이 외에 RGD 섭취, 경색심근의 크기와 그 변화, 자가방사촬영 및 면역병리염색결과에서 bFGF 치료군과 생리식염수 주입군 사이에 유의한 차이는 보이지 않았다.

결론: ^{68}Ga-RGD 는 경색심근에 섭취가 증가함으로써 심근경색영상화의 가능성을 보여 주었다. 심근 내에 bFGF 일회 투여가 단기간의 혈관신생 증가에 도움이 되는 것을 ^{68}Ga-RGD PET 으로 확인할 수 있었으나 장기적인 효과는 없어 장기적인 예후에는 도움이 크지 않을 것임을 시사하였다. ^{68}Ga-RGD 는 심근경색 영상과 혈관신생치료 효과를 평가하는 영상 추적자로 유용할 것으로 기대된다.

중심단어: 심근경색, 치료적 혈관신생, 분자영상, ^{68}Ga, RGD 펩티드, 양전자단층촬영

학 번: 2006-30507